minerals

MDPI

Article

Utilization of Ammonium Chloride as a Novel Selective Depressant in Reverse Flotation of Potassium Chloride

Runqing Liu [1,2], Hongyu Lu [1,2], Li Wang [1,2,*], Mengjie Tian [1,2] and Wei Sun [1,2,*]

[1] School of Minerals Processing and Bioengineering, Central South University, Changsha 410083, China; liurunqing@126.com (R.L.); luhongyuxu@163.com (H.L.); 15200826490@163.com (M.T.)

[2] Key Laboratory of Hunan Province for Clean and Efficient Utilization of Strategic Calcium-containing Mineral Resources, Central South University, Changsha 410083, China

* Correspondence: li_wang@csu.edu.cn (L.W.); sunmenghu@csu.edu.cn (W.S.); Tel.: +86-731-88830482 (L.W. & W.S.); Fax: +86-0731-88660477 (L.W. & W.S.)

Received: 14 November 2018; Accepted: 10 January 2019; Published: 13 January 2019

Abstract: The separation of sylvite (KCl) and halite (NaCl), two main minerals in potash ores, is difficult because of the high ion concentration, fine particles of NaCl, and aggregation of KCl and NaCl in the saturated system. This study employed ammonium chloride (NH_4Cl) as a new depressant and dodecyl morpholine as a collector in the reverse flotation process. The depressing mechanisms were studied by adsorption capacity experiments, infrared spectral analysis, and molecular dynamics simulations. The flotation tests showed that NaCl recovery increased to 97% after the addition of NH_4Cl, while KCl recovery was reduced to <1%. Notably, NH_4Cl not only acted as a selective KCl depressant, but also activated NaCl flotation. The FTIR measurements showed that NH_4Cl was physically adsorbed onto the KCl and NaCl surfaces. Adsorption capacity experiments and molecular dynamics simulations confirmed more favorable NH_4Cl adsorption on the KCl surface than on the NaCl surface. Moreover, the KCl mineral surface was more hydrophilic, while that of NaCl was more hydrophobic. Relative concentration analysis revealed that >90% ammonium and chloride ions were distributed 2–10 Å away from the KCl surface but were dispersed on the NaCl surface, indicating that NH_4Cl exhibited stronger intermolecular interactions with KCl than with NaCl.

Keywords: KCl; NaCl; NH_4Cl; flotation; molecular dynamics simulations

1. Introduction

Potash is a significant raw material in medicine, food, and other chemical industries and is most notably used as a fertilizer in agriculture [1,2]. Among all the mineral salt species used in sylvite (KCl) production, halite (NaCl) separation is very difficult because of its high ion concentration, fine particles, and its aggregation with KCl in a saturated system. Thus, globally, most potash ores are concentrated by froth flotation [3]. In this process, direct flotation collectors comprise alkyl fatty amines [4] and alkyl sulfonates [5], while reverse flotation collectors contain carboxylic acids [6], amides [7], and morpholines [8].

Previous studies [9,10] have shown that in the flotation of KCl, aliphatic primary amines with C12–C18 carbon chain lengths exhibit better flotation and the flotation effect improves as the carbon chain length increases. Currently, over 80% of the world's potash is produced by the selective flotation of KCl from NaCl and other gangue minerals using long-chain (C16–C22 aliphatic chains) amine collectors, as observed in potash mining in Saskatchewan [11]. However, the process of eliminating the C16–C22 long-chain amines is relatively harsh and comprises melting at temperatures in the range 70–90 °C and neutralization with hydrochloric or acetic acids [12]. In the actual flotation process, the amine collector of the KCl concentrate products afforded smaller granularity, captured NaCl fine particles to concentrate the products, and degraded the quality of the concentrate, thereby hindering the production of highly pure KCl. Alkylmorpholine has been employed as a reverse flotation collector of KCl. Alkylmorpholine sorption at the halite surface proceeds with high selectivity, creating the conditions necessary for efficient and selective flotation separation of NaCl and KCl [8]. This process does not require the addition of auxiliary agents and shows relatively good flotation index [13]. Currently, the reverse flotation method is being applied in the potash industry, including operations in the Dead Sea (Israel and Jordan), Verkhnekamskoye (Russia), and Chaerhan Salt Lake (Qinghai province, China). Dodecyl morpholine (DMP) was used as a collector to float NaCl from carnallite in the Qinghai Salt Lake Group operations, whereby ~50 g/t carnallite feed was employed. The flotation recovery of NaCl was ~90%, while the KCl grade in the final product was in the range 90–95%, with an overall KCl recovery of 59–62% [13]. However, dodecyl morpholine continues to carry KCl during flotation. Thus, for industries with high-quality KCl requirements, obtaining high-quality KCl products remains a problem.

Alkyl amines, which are used as direct flotation collectors, are selectively adsorbed onto KCl [14,15]. Thus, it follows that NH_4Cl can also be effectively adsorbed onto the KCl surface because its ammonium ion is similar to the alkyl ammonium ion. However, the alkyl amine hydrophobic carbon chains increase the hydrophobicity of the mineral surface. Hence, the KCl surface is more hydrophilic after the addition of NH_4Cl because this depressant does not comprise a hydrophobic carbon chain and its chloride ion is hydrophilic. Thus, NH_4Cl is the ideal KCl depressor in theory. In this study, the effect of NH_4Cl as a depressor in the DMP flotation of KCl was elucidated. Furthermore, the mechanism of NH_4Cl adsorption was investigated through adsorption experiments, infrared spectroscopy, and molecular dynamics (MD) simulations.

2. Experimental

2.1. Materials and Reagents

Analytically pure KCl and NaCl samples were used as pure minerals. Both samples were dry ground and sieved. The fractions of pure KCl and NaCl with the particle sizes 165–200 μm and <200 μm, respectively, were obtained as flotation samples and used as single minerals. The X-ray powder diffraction spectra revealed that the purities of the KCl and NaCl samples were 98% and 99%, respectively. Both minerals were ground in a ceramic ball mill and the fractions in the size range 38–74 μm were used in the flotation tests. Deionized water with a resistivity >18 MΩ·cm was used in all the experiments. The reagents used in the study are listed in Table 1.

Table 1. Reagents used in experiments.

Chemical	Concentration	Supplier	Role
KCl	98%	Sinopharm Chemical Reagent Co., Ltd., Beijing, China	Pure minerals
NaCl	99%	Sinopharm Chemical Reagent Co., Ltd., Beijing, China	Pure minerals
$MgCl_2\cdot 6H_2O$	99%	Sinopharm Chemical Reagent Co., Ltd., Beijing, China	Preparation of saturated brine
$CaSO_4\cdot 2H_2O$	99%	Sinopharm Chemical Reagent Co., Ltd., Beijing, China	Preparation of saturated brine
NH4Cl	99%	Sinopharm Chemical Reagent Co., Ltd., Beijing, China	Regulator
DMP	-	In-house	Collector

The saturated brines were prepared by dissolving a sufficient amount of salt (Table 2) in Millipore water with stirring for 2 h. The saturated solutions were then stored at room temperature for 24 h and filtered before use. The DMP solution (0.01 g/L, 99% purity) was prepared in the laboratory with saturated brine as the solvent. Flotation tests were conducted using DMP as the collector and NH_4Cl as the regulator. All the reagents used in the tests were of analytical grade.

Table 2. Ingredients of salt brine.

Composition	**$MgCl_2$**	**NaCl**	**KCl**	**$CaSO_4$**	**H_2O**
Content (%)	33.60	0.55	0.37	0.14	65.34

2.2. Flotation Tests

The single-mineral flotation KCl and NaCl tests were conducted on an XFG flotation machine (Exploring Machinery Plant, Changchun, China) with a volume of 50 mL and an impeller speed of 1850 rpm (Figure 1). A well-configured and filtered saturated brine solution was used as the flotation medium. In each test, 10 g mineral sample and 40 mL saturated brine solution were added in the cell and conditioned for 3 min. The flotation experiment was divided into two parts: first, the suspension was dosed with 900–1500 g/t DMP as the collector. Subsequently, to test the effect of NH_4Cl, the prepared NH_4Cl was applied before adding the optimal DMP dosage. The depressant (if needed) and collector were added sequentially and conditioned for 5 and 10 min, respectively. After 10 min of flotation, the products were collected, dried, and weighed and the recovery was then calculated. The flotation flowsheet is displayed in Figure 2. Each flotation test was conducted in triplicate and the average was reported as the final value. The standard deviation, which is presented as an error bar, was obtained from the mean of the three measurements per experimental condition.

Figure 1. Schematic of the XFG series flotation machine.

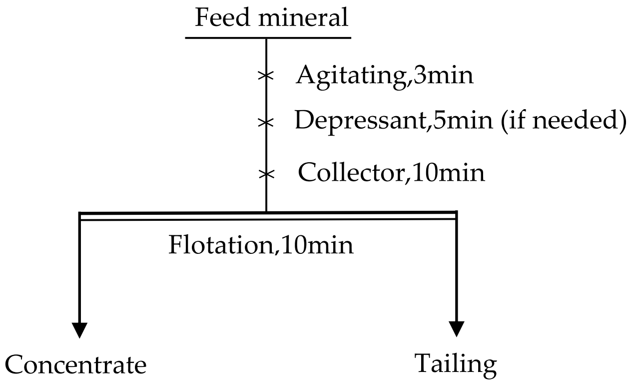

Figure 2. Flowsheet of the single-mineral flotation tests.

2.3. Adsorption Measurements

The adsorption measurements were completed using a total organic carbon analyzer (TOC-L CPH/CPN, Shimadzu Corporation, Kyoto, Japan). Different dosages were used as the dosing conditions, while a saturated salt brine solution with no added minerals was set as the reference group. A total of 10 g mineral was added to the experimental group, while no minerals were added to the reference group. The volume of the entire slurry was maintained at 40 mL after the addition of the mineral (in different dosages). All the pulp was placed in a clean beaker and stirred in a magnetic stirrer for 15 min, after which the supernatant was withdrawn. The sample was diluted four-fold in a 50 mL PET tube and centrifuged for 15 min at a speed of 18,000 rpm to determine the total amount of organic carbon. The experiments were repeated at least in triplicate and the average data were plotted. The standard deviation, presented as an error bar, was obtained using the mean of the three measurements per experimental condition. The adsorption of the reagent on the mineral surface was calculated as follows [16,17]:

$$\Gamma = \frac{m_1 - m_2}{m}, \tag{1}$$

where Γ is the adsorption amount, μg/g mineral; m_1 is the weight of total reagent in the solution measured in the reference group, μg; m_2 is the weight of total reagent in the solution measured in the experimental group, μg; and m is the weight of the mineral, g.

2.4. Infrared Spectral Analysis

Fourier-transform infrared spectroscopy (FTIR, Bio-Rad FTS-6000, Cambridge, MA, USA) was performed at room temperature in the range 4000–400 cm^{-1}. After the pure minerals were conditioned with the reagents in the solution, the samples were filtered naturally, dried thoroughly in a vacuum oven at 40 °C, and ground to <2 μm in an agate mortar. The spectra of the solids were recorded using KBr pellets.

2.5. MD Simulations

The adsorption behavior of the ammonium ions on the NaCl (100) and KCl (001) surfaces was explored by MD simulation. The initial adsorption models were built using the software package, Materials Studio 6.0 (Dassault Systèmes BIOVIA, San Diego, CA, USA). The condensed-phase optimized molecular potentials for atomic simulation studies (COMPASS) force-field was used to calculate the inter- and intra-atomic interactions. Additionally, density functional theory calculations for the ammonium ion, NaCl (100) surface, and KCl (001) surface were implemented to assign the charges in the CASTEP module. The Perdew-Burke-Ernzerhof functional with a generalized gradient approximation was used throughout the study.

Based on the natural cleavage plane reported in previous studies [18,19], the NaCl and KCl mineral surfaces were built to construct the adsorption models. After the mineral surface models were built, the amorphous cell, a packing module, was used for the construction of the reagent matrix on the surfaces. The chloride ions were added to maintain the system neutral. A strict reagent addition sequence (Figure 1) was adopted. The built vacuum slab (thickness ca. 80 Å) eliminated the influence of the period boundary conditions. During the simulation, the ammonium and chloride ions in the solution moved freely, while the NaCl and KCl sheets were fixed.

Molecular optimization was carried out using a Smart Minimizer to eliminate the possible overlap of molecules during the process of building the configuration. The simple point-charge model was used to simulate liquid water. The temperature was controlled by an Andersen thermostat. The canonical (NVT) ensemble was applied at the temperature 298 K for each system using a Nosé-Hoover thermostat, while the integration step was set at 1 fs. Finally, each system was simulated for 4 ns to reach the equilibrium state and the last 1 ns of each trajectory was used for the analysis.

3. Results and Discussion

3.1. NH_4Cl as a Depressant for KCl and NaCl

Figure 3a illustrates the effect of the DMP dosage on the flotation of KCl and NaCl in the absence of NH_4Cl. In this flotation system, the NaCl exhibited good flotability, while KCl presented a very poor flotation ability in the presence of the DMP collector. Further, with an increase in the collector dosage, in the range 900–1400 g/t, the flotation recovery increased monotonically and a maximum value of 93.13% NaCl recovery was achieved at 1400 g/t DMP. In the test dosage range 900–1500 g/t, the flotation recoveries of NaCl and KCl were >70% and <4.5%, respectively. Comparatively, typical recoveries achieved in some of the flotation plants in Saskatchewan, which used long-chain amines as collectors, were in the range 85–88% [11]. Qinghai Avic Resources Co., Ltd., in Mahai also employed traditional KCl flotation from NaCl with an amine as the collector to produce the final KCl product in the grade range 86–92% [13]. In this experiment, the loss of KCl was >10% when long-chain amines were used as collectors, exceeding the maximum value (4.5%) of KCl loss rate. This indicates that DMP exhibits a good selective collecting ability for NaCl and can be utilized to separate NaCl from KCl.

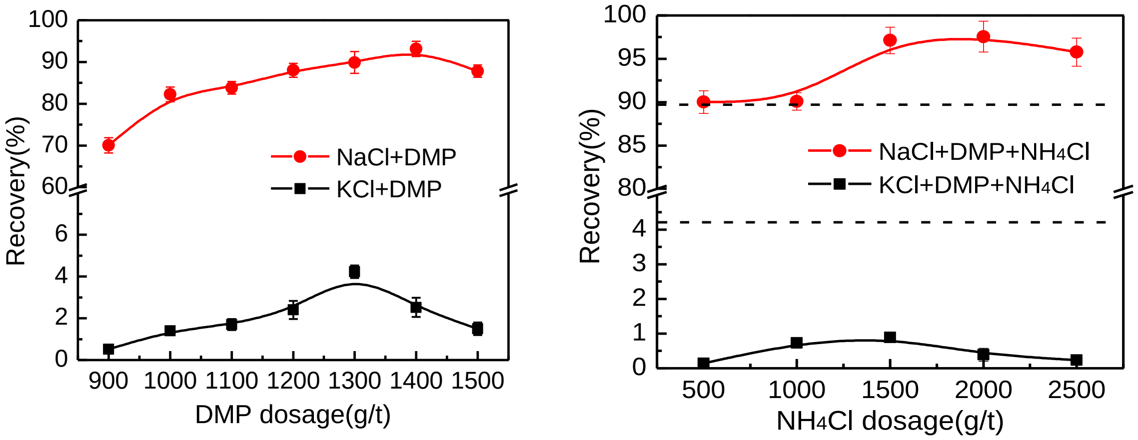

(a) (b)

Figure 3. (**a**) Effect of the DMP dosage on the recovery of KCl and NaCl and (**b**) effect of NH_4Cl dosage on the recovery of KCl and NaCl in the presence of DMP.

The flotation response was significantly different when NH_4Cl was employed as the depressant. Figure 3b illustrates the effect of NH_4Cl dosage on the flotation of KCl and NaCl in the presence of DMP. The DMP dosage was fixed at 1300 g/t, the optimal dosage in the DMP flotation system. The KCl and NaCl recoveries were 4.23% and 89.88%, respectively, in the absence of NH_4Cl. After the addition of NH_4Cl, the flotation of KCl was inhibited, while the recovery was <1% in the test dosage range 500–2500 g/t. Interestingly, NH_4Cl did not depress the flotation of NaCl but showed an activation effect on NaCl. The recovery of NaCl increased with an increase in the NH_4Cl dosage and reached a maximum value of 97.55% at an NH_4Cl dosage of 2000 g/t, indicating that NH_4Cl promoted the flotation separation of NaCl and KCl with DMP as a collector.

3.2. Adsorption Capacity Experiments

Figure 4a presents the adsorption capacity of DMP on the NaCl and KCl surfaces. DMP adsorption was significantly higher onto the NaCl surface than on the KCl surface. The adsorption of DMP onto KCl and NaCl gradually increased and reached maximum values at dosages of 1300 and 1400 g/t, respectively. These values agree with the flotation experiment results. Figure 4b illustrates that in the dosage range tested (500–2500 g/t), the adsorption capacity of NH_4Cl onto the KCl surface was significantly higher than onto the NaCl surface. The adsorption amount of NH_4Cl onto the KCl surface was about 50 μg/g higher than that on the NaCl surface and increased with an increase in the NH_4Cl dosage. The difference between the adsorption amounts of the two minerals reached a maximum of 71.9 μg/g at the NH_4Cl dosage 2500 g/t.

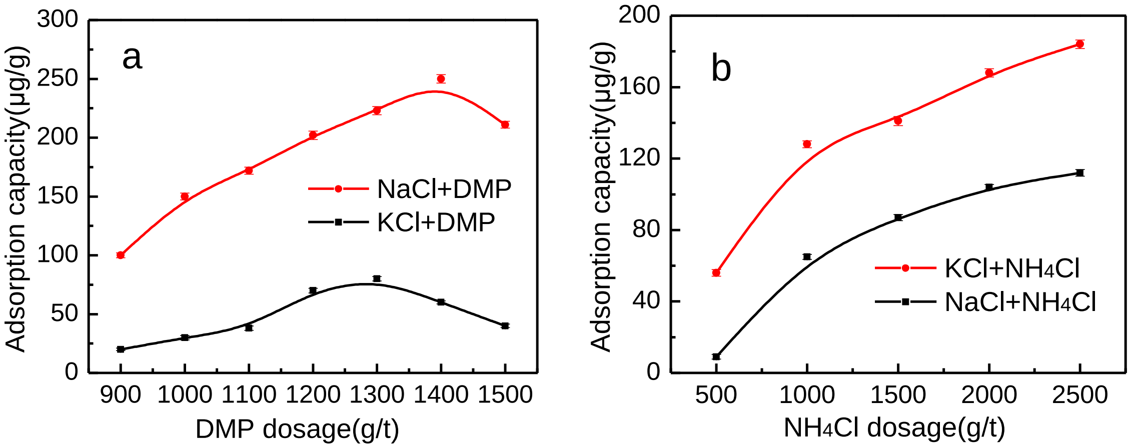

Figure 4. Absorption capacity of (**a**) DMP and (**b**) NH_4Cl on the KCl and NaCl surfaces.

3.3. FTIR Spectroscopy Analysis

FTIR is commonly used to characterize the mechanism of the reaction between a mineral and a reagent. The FTIR spectra of NH_4Cl, KCl, and KCl reacted with NH_4Cl are presented in Figure 5. In the NH_4Cl spectrum, the characteristic sharp band near 3137 cm^{-1} corresponds to the stretching N–H vibration, while the band near 1402 cm^{-1} was assigned to the flexural vibration of the ammonium ion [20]. After the reaction between KCl and NH_4Cl (Figure 5c), characteristic sharp bands near 1404 and 3137 cm^{-1} on the KCl surface, corresponding to the flexural vibration of the ammonium ion and the N–H stretching vibration, respectively, were observed. After treatment with NH_4Cl (Figure 5e), peaks from ammonium ion flexural and N–H stretching vibrations were also observed, suggesting that NH_4Cl adsorbed onto the NaCl surface. The spectra of NH_4Cl-treated KCl (Figure 5c) and NaCl (Figure 5e) exhibited absorption peaks characteristic of NH_4Cl. However, no band shift was observed, indicating that the adsorption of NH_4Cl on KCl and NaCl is dominated by physical adsorption.

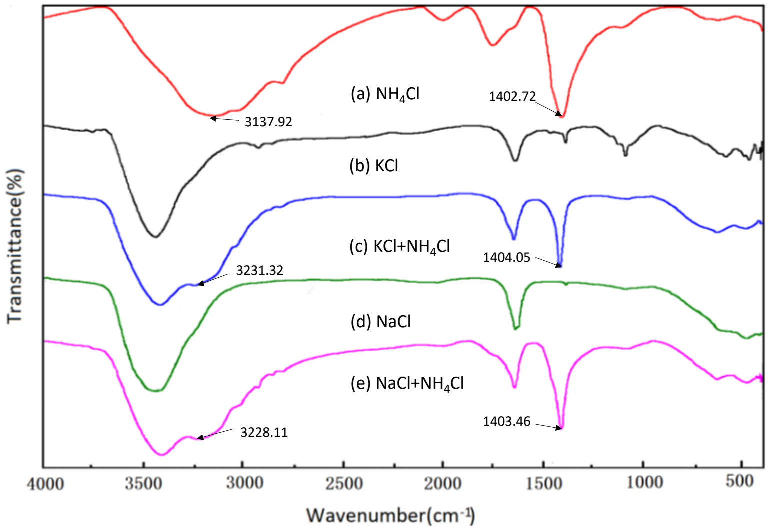

Figure 5. FTIR spectra of (**a**) NH_4Cl, (**b**) KCl, (**c**) KCl+NH_4Cl, (**d**) NaCl, and (**e**) NaCl+NH_4Cl.

The DMP FTIR spectra are presented in Figure 6a. The bands at 2922 and 2852 cm^{-1} were assigned to the C–H stretching vibration [21,22]. Moreover, weak characteristic peaks of DMP at 3026 and 2802 cm^{-1} were detected on the KCl surface under the precondition that NH_4Cl reacted with KCl, suggesting that small amounts of DMP adsorbed onto the KCl surface. The characteristic peaks of DMP at 3029 and 2802 cm^{-1} were still significant in the NaCl+NH_4Cl spectrum (Figure 6e), indicating that DMP was effectively adsorbed onto the NaCl surface in the presence of NH_4Cl. Based on these results, it can be concluded that significantly strong physical adsorption of DMP occurs on the NaCl surface after treatment with NH_4Cl. On the other hand, DMP hardly adsorbs on the NH_4Cl-treated KCl surface. These FTIR results support the flotation results.

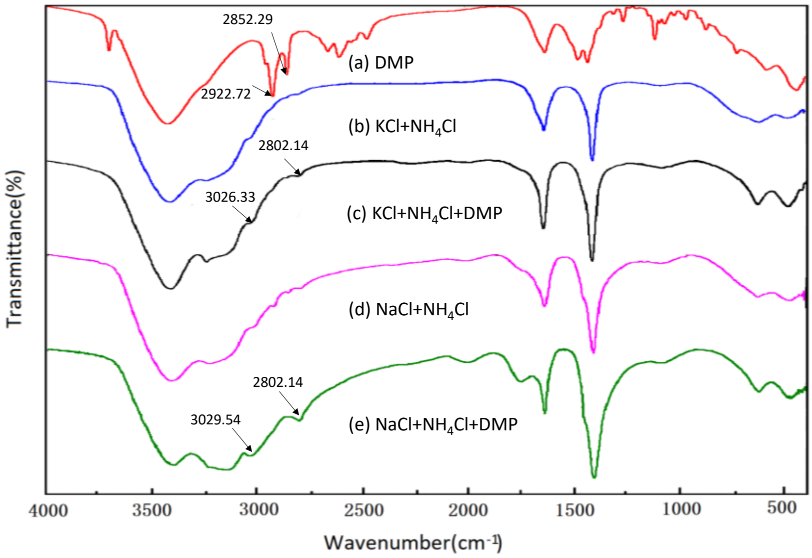

Figure 6. FTIR spectra of (**a**) DMP, (**b**) KCl+NH_4Cl, (**c**) KCl+NH_4Cl+DMP, (**d**) NaCl+NH_4Cl, and (**e**) NaCl+NH_4Cl+DMP.

3.4. Computation Results by MD Simulations

3.4.1. NH_4Cl Adsorption States on the NaCl and KCl Crystal Surfaces in Vacuum

MD simulation was used to investigate the solid-liquid interface properties and determine the micro-adsorption structure on a molecular scale [23–26]. Studies have reported that NH_4Cl adsorbs on KCl through the chloride ions, which act with the surface potassium atoms. Figure 7 presents the models of the mineral–reagent complex after NH_4Cl adsorption in vacuum. Almost all the chloride ions absorbed onto the KCl surface and interacted strongly with the potassium atoms. Moreover, the ammonium ions were also close to the KCl surface, probably because of their interaction with the surface chloride ions and the chlorine atoms in the KCl crystal. On the other hand, in the NaCl system (Figure 7b), the ammonium and chloride ions were alienated from the surface and did not collect at the NaCl surface.

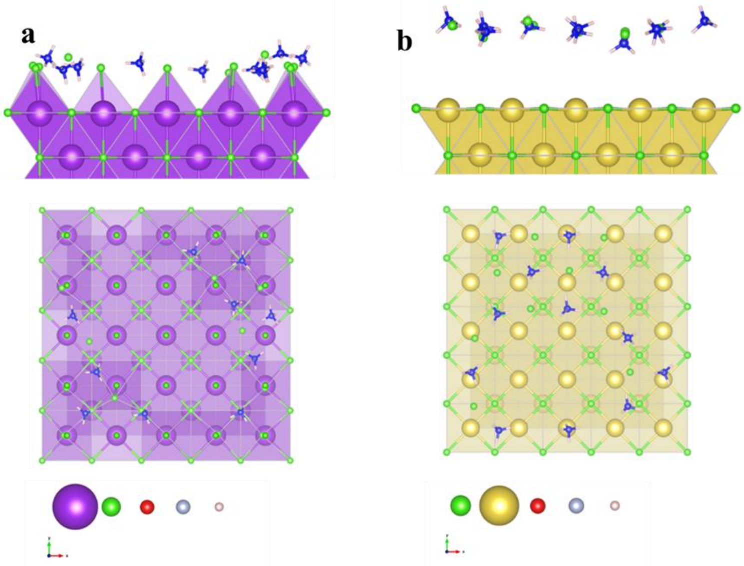

Figure 7. Front and top view snapshots of nine ammonium and chloride ions near the (**a**) KCl surface in vacuum and (**b**) NaCl surface in vacuum. The color scheme is as follows: red, oxygen atoms; white, hydrogen atoms; blue, nitrogen atoms; purple, potassium atoms; yellow, sodium atoms; and green, chlorine atoms.

3.4.2. NH_4Cl Adsorption States on the NaCl and KCl Crystal Surfaces in the Presence of Water Molecules

Retaining the original vacuum condition, 200 water molecules were added to the system to investigate the effects of the ammonium and chloride ions on the KCl and NaCl surfaces in the presence of water as well as the hydrophilicity and hydrophobicity of the two minerals. Figure 8a illustrates that the ammonium and chloride ions interacted strongly with KCl and were effectively adsorbed onto the mineral surface. On the other hand, in the KCl system, the water molecules were close to the mineral surface because KCl is hydrophilic. The data in Figure 8b revealed that in the presence of water molecules, the ammonium and chloride ions were further away from the NaCl surface because of the hydrophobicity of NaCl. The above conditions were consistent with those observed under vacuum conditions and validated the conclusion reached on flotation.

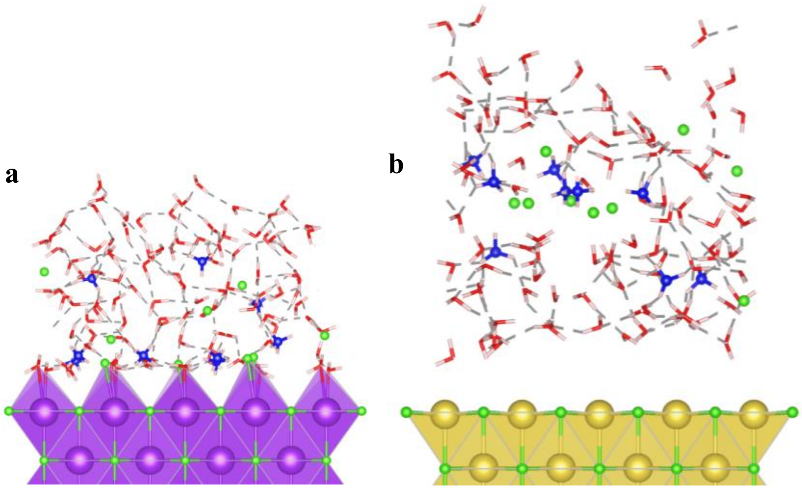

Figure 8. MD simulation snapshot of ammonium and chloride ions near the (**a**) KCl and (**b**) NaCl surfaces with 200 water molecules each. The color scheme is as follows: red, oxygen atoms; white, hydrogen atoms; blue, nitrogen atoms; purple, potassium atoms; yellow, sodium atoms; and green, chlorine atoms.

The analysis of the relative concentrations of the reagents as a function of distance from the mineral surface provided a quantitative basis for the adsorption ability [27]. The NH_4Cl distribution on different minerals could therefore be quantified by calculating the relative concentrations of the ammonium and chloride ions [28]. The concentration profiles along the *z*-axis were calculated with the normal *z*-axis on the mineral surface set as the zero point (Figure 9). After the interaction of NH_4Cl with KCl, the ammonium and chloride ions were both distributed at distances in the range 2–13 Å from the KCl surface and 2–19 Å from the NaCl surface. The relative concentrations of the ammonium ions in the range 3–8 Å away from the KCl surface are all >10%, while the maximum relative concentration of ammonium ions 9.46 Å away from the NaCl surface is <10%. Moreover, >90% ammonium ions and chloride ions were distributed 2–10 Å away from the KCl surface. However, these ions were dispersed on the NaCl surface, indicating that NH_4Cl exhibited a stronger intermolecular interaction with KCl than with NaCl. The relative concentration distribution of the chloride ions on the KCl and NaCl surfaces was similar to that of the ammonium ions. In the aqueous solution system, analysis of the relative concentration results revealed that the ammonium and chloride ions were close to the KCl surface, indicating that the strong interaction between NH_4Cl and KCl led to the strong adsorption of the former mineral onto the mineral surface. Conversely, the ammonium and chloride ions were far from the NaCl surface, indicating that NH_4Cl exhibited a weaker intermolecular interaction with NaCl than with KCl. The results of the MD simulations verified the flotation results.

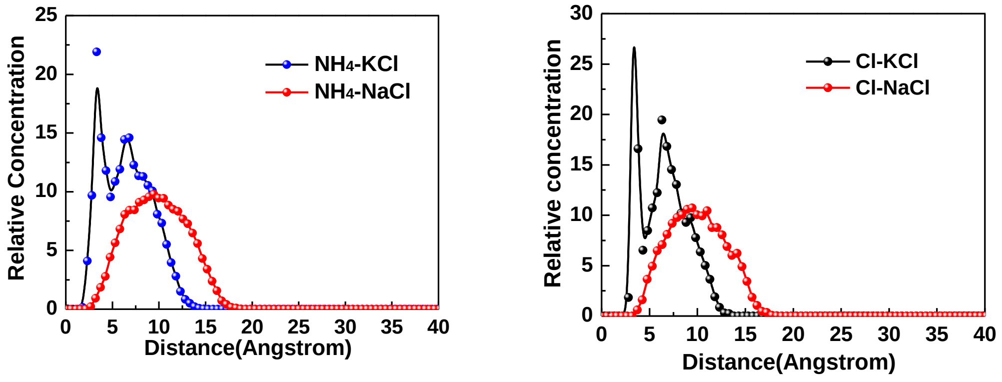

(a) (b)

Figure 9. The *z*-direction relative concentration of the (**a**) ammonium ions and (**b**) chloride ions.

The simulation results in this study were consistent with the surface charge theory [29], where the governing mechanism for soluble salt flotation comprised the electrostatic interaction between the salt surface and the collector species [30]. In the surface charge theory, KCl and NaCl carry opposite charges, KCl being negatively charged and NaCl being positively charged in their saturated brines. These speculations were later confirmed by the nonequilibrium electrophoretic mobility measurements [31]. Therefore, the flotation separation of KCl from NaCl was achieved because of the adsorption of cationic surfactants such as C12–C18 amine ions or positively charged collector colloids on the negatively charged KCl surface but not on the positively charged NaCl surface [31,32]. MD simulation results revealed that the adsorption of chloride ions onto the KCl surface resulted in a negatively charged KCl surface. The results verified the above theory that the KCl surface was negatively charged; thus, ammonium ions were adsorbed onto the negatively charged KCl surface by electrostatic attraction and alienated the positively charged NaCl surface because of electrostatic repulsion.

4. Conclusions

Dodecyl morpholine is a selective collector for the flotation of NaCl and KCl. Reverse flotation is being applied in the industry and is more effective than traditional flotation, which employs long-chain ammonium compounds as collectors [13,33]. The addition of NH_4Cl promoted the separation of KCl and NaCl. The flotation tests revealed that NH_4Cl exerts a considerable inhibitory effect on KCl so that the recovery was reduced to <1%. It also exhibited a significant activation effect on NaCl so that the maximum recovery value was 97.55%.

The adsorption experiments and FTIR measurements indicated that DMP adsorption was significantly higher on the NaCl surface than on the KCl surface. However, the adsorption of NH_4Cl onto the KCl surface was stronger than that on the NaCl surface and the difference increased with an increase in the NH_4Cl dosage. The characteristic DMP peaks at ~3029 cm^{-1} and ~2802 cm^{-1} were still significant on the NaCl surface. On the other hand, the characteristic peaks detected on the KCl surface in the presence of NH_4Cl were weak. Notably, NH_4Cl and DMP were physically adsorbed onto the surfaces of both minerals.

MD simulations demonstrated that the adsorption of NH_4Cl onto the KCl surface was very strong because of the presence of electrostatic forces. However, NH_4Cl displayed weak interactions with NaCl and could not be adsorbed onto the NaCl surface. In an aqueous solution system, the KCl surface was hydrophilic, while the NaCl surface was hydrophobic. The relative concentration measurements indicated that the ammonium and chloride ions were close to the KCl surface but far away from that of NaCl, indicating that NH_4Cl exhibited stronger interactions with KCl than with NaCl; this led to its stronger adsorption onto the KCl surface. The results in this study therefore confirmed that NH_4Cl promotes the flotation separation of NaCl and KCl with DMP as the collector.

Author Contributions: Conceptualization, R.L. and L.W.; Methodology, L.W.; Software, M.T.; Validation, L.W., M.T.; Formal Analysis, H.L.; Investigation, R.L.; Resources, W.S.; Data Curation, H.L.; Writing-Original Draft Preparation, H.L.; Writing-Review & Editing, R.L. and H.L.; Visualization, H.L.; Supervision, W.S.; Project Administration, R.L.; Funding Acquisition, W.S.

Funding: This study was financially supported by the Collaborative Innovation Center for Clean and Efficient Utilization of Strategic Metal Mineral Resources, the National 111 Project (No. B14034), and the Key Laboratory of Hunan Province for Clean and Efficient Utilization of Strategic Calcium-containing Mineral Resources (No. 2018TP1002).

Acknowledgments: We would like to thank the Central South University for providing us with the experimental platform.

Conflicts of Interest: The authors declare no conflict of interest.

References

1. Li, E.; Du, Z.; Yuan, S.; Cheng, F. Low temperature molecular dynamic simulation of water structure at sylvite crystal surface in saturated solution. *Miner. Eng.* **2015**, *83*, 53–58. [CrossRef]
2. Larsson, S.; Gustafsson, G.; Häggblad, H.-Å.; Jonsén, P. Experimental and numerical study of potassium chloride flow using smoothed particle hydrodynamics. *Miner. Eng.* **2018**, *116*, 88–100. [CrossRef]
3. Ozdemir, O.; Karakashev, S.I.; Nguyen, A.V.; Miller, J.D. Adsorption and surface tension analysis of concentrated alkali halide brine solutions. *Miner. Eng.* **2009**, *22*, 263–271. [CrossRef]
4. Cao, Q.; Du, H.; Miller, J.D.; Wang, X.; Cheng, F. Surface chemistry features in the flotation of KCl. *Miner. Eng.* **2010**, *23*, 365–373. [CrossRef]
5. Du, H.; Ozdemir, O.; Wang, X.; Cheng, F.; Celik, M.S.; Miller, J.D. Flotation chemistry of soluble salt minerals: From ion hydration to colloid adsorption. *Miner. Metall. Process.* **2014**, *31*, 1–20. [CrossRef]
6. Wachsmuth, U.; Brod, J. Process for the Selective Flotation of Kainite from Mineral Mixtures Using Sulfated Fatty Acids as the Collector Reagent. U.S. Patent 20170361335A1, 21 December 2017.
7. Berthon, R.; Mames, M.; Zimmerman, J.-P. Amine-amide collectors for the treatment of potash ores. U.S. Patent 3596763, 3 August 1971.
8. Titkov, S.; Sabirov, R.; Panteleeva, N. Investigations of alkylmorpholines—–Collectors for a new halite flotation process. *Miner. Eng.* **2003**, *16*, 1161–1166. [CrossRef]
9. Monte, M.; Oliveira, J. Flotation of sylvite with dodecylamine and the effect of added long chain alcohols. *Miner. Eng.* **2004**, *17*, 425–430. [CrossRef]
10. Laskowski, J.; Castro, S. Flotation in concentrated electrolyte solutions. *Int. J. Miner. Process.* **2015**, *144*, 50–55. [CrossRef]
11. Perucca, C.F. Potash processing in Saskatchewan—A review of process technologies. *CIM Bull.* **2003**, *96*, 61–65.
12. Wu, Z.; Wang, X.; Liu, H.; Zhang, H.; Miller, J.D. Some physicochemical aspects of water-soluble mineral flotation. *Adv. Colloid Interface Sci.* **2016**, *235*, 190–200. [CrossRef]
13. Wang, X.; Miller, J.D.; Cheng, F.; Cheng, H. Potash flotation practice for carnallite resources in the Qinghai Province, PRC. *Miner. Eng.* **2014**, *66–68*, 33–39. [CrossRef]
14. Ozdemir, O.; Du, H.; Karakashev, S.I.; Nguyen, A.V.; Celik, M.S.; Miller, J.D. Understanding the role of ion interactions in soluble salt flotation with alkylammonium and alkylsulfate collectors. *Adv. Colloid Interface Sci.* **2011**, *163*, 1–22. [CrossRef] [PubMed]
15. Laskowski, J.S. From amine molecules adsorption to amine precipitate transport by bubbles: A potash ore flotation mechanism. *Miner. Eng.* **2013**, *45*, 170–179. [CrossRef]
16. Liu, X.; Xie, J.; Huang, G.; Li, C. Low-temperature performance of cationic collector undecyl propyl ether amine for ilmenite flotation. *Miner. Eng.* **2017**, *114*, 50–56. [CrossRef]
17. Yin, W.; Yang, B.; Fu, Y.; Chu, F.; Yao, J.; Cao, S.; Zhu, Z. Effect of calcium hypochlorite on flotation separation of covellite and pyrite. *Powder Technol.* **2019**, *343*, 578–585. [CrossRef]
18. Zhang, Y.; Hu, Y.; Sun, N.; Liu, R.; Wang, Z.; Wang, L.; Sun, W. Systematic review of feldspar beneficiation and its comprehensive application. *Miner. Eng.* **2018**, *128*, 141–152. [CrossRef]
19. Xu, L.; Tian, J.; Wu, H.; Fang, S.; Lu, Z.; Ma, C.; Sun, W.; Hu, Y. Anisotropic surface chemistry properties and adsorption behavior of silicate mineral crystals. *Adv. Colloid Interface Sci.* **2018**, *256*, 340–351. [CrossRef]
20. Maiti, K.S. Ultrafast N–H vibrational dynamics of hydrogen-bonded cyclic amide reveal by 2DIR spectroscopy. *Chemical Physics* **2018**, *515*, 509–512. [CrossRef]
21. Mal, N.K.; Kumar, P.; Fujiwara, M. Sorption properties and hydrothermal stability of MCM-41 prepared by pH adjustment and salt addition. In *Studies in Surface Science and Catalysis*; Sayari, A., Jaroniec, M., Eds.; Elsevier: Amsterdam, The Netherlands, 2002; Volume 141, pp. 445–452.
22. Liu, D.Y.; Sui, G.X.; Bhattacharyya, D. Properties and characterization of electrically conductive nanocellulose-based composite films. In *Fillers and Reinforcements for Advanced Nanocomposites*; Dong, Y., Umer, R., Lau, A.K.-T., Eds.; Woodhead Publishing: Sawston, UK, 2015; pp. 3–25.
23. Leermakers, F.A.M.; Koopal, L.K.; Goloub, T.P.; Vermeer, A.W.P.; Kijlstra, J. Confinement-Induced Symmetry Breaking of Interfacial Surfactant Layers. *J. Phys. Chem. B* **2006**, *110*, 8756–8763. [CrossRef]
24. Reimer, U.; Wahab, M.; Schiller, P.; Moegel, H.J. Monte Carlo study of surfactant adsorption on heterogeneous solid surfaces. *Langmuir* **2005**, *21*. [CrossRef]

25. Tarek, M.; Bandyopadhyay, S.; Klein, M.L. Molecular dynamics studies of aqueous surfactants systems. *J. Mol. Liq.* **1998**, *78*, 1–6. [CrossRef]
26. Wang, L.; Sun, N.; Wang, Z.; Han, H.; Yang, Y.; Liu, R.; Hu, Y.; Tang, H.; Sun, W. Self-assembly of mixed dodecylamine–dodecanol molecules at the air/water interface based on large-scale molecular dynamics. *J. Mol. Liq.* **2019**, *276*, 867–874. [CrossRef]
27. Jang, C.; Lacy, T.E.; Gwaltney, S.R.; Toghiani, H.; Pittman, C.U. Interfacial shear strength of cured vinyl ester resin-graphite nanoplatelet from molecular dynamics simulations. *Polymer* **2013**, *54*, 3282–3289. [CrossRef]
28. Li, L.; Hao, H.; Yuan, Z.; Liu, J. Molecular dynamics simulation of siderite-hematite-quartz flotation with sodium oleate. *Appl. Surf. Sci.* **2017**, *419*, 557–563. [CrossRef]
29. Miller, J.D.; Yalamanchili, M.R. Fundamental aspects of soluble salt flotation. *Miner. Eng.* **1994**, *7*, 305–317. [CrossRef]
30. Roman, R.J.; Fuerstenau, M.C.; Seidel, D.C. Mechanisms of soluble salt flotation. I. *Trans. Am. Inst. Min. Metall. Petrol. Eng.* **1968**, *241*, 56–64.
31. Miller, J.D.; Yalamanchili, M.R.; Kellar, J.J. Surface charge of alkali halide particles as determined by laser-Doppler electrophoresis. *Langmuir* **1992**, *8*, 1464–1469. [CrossRef]
32. Yalamanchili, M.R.; Kellar, J.J.; Miller, J.D. Adsorption of collector colloids in the flotation of alkali halide particles. *Int. J. Min. Process.* **1993**, *39*, 137–153. [CrossRef]
33. Pan, B. *Flotation of Halite and Sylvite from Carnallite with Dodecyl Morpholine*; The University of Utah: Salt Lake City, UT, USA, 2013.